MICROHARDNESS AND MICROSTURCTURE EVALUATION OF PREHEATED STEEL G550 THROUGH MICROWAVE HYBRID HEATING

Shamini Janasekaran, Walisijiang. Tayier and Mohamed Nabil Awad

Center for Advanced Materials and Sustainable Manufacturing, Faculty of Engineering, Built Environment & Information Technology, SEGi University, Petaling Jaya 47810, Selangor, Malaysia.

*shaminijanasekaran@segi.edu.my

Abstract. Microwave hybrid heating represents an innovative approach to preheating materials. Previous research has investigated the heat transfer of various metallic materials, including steel, copper, and aluminium. However, achieving high heat temperatures has been a challenge due to the limited power output of microwave sources used in heating techniques. In this study, steel G550 sheets (20 x 20 x 0.6 mm) were preheated using a novel microwave heating technique within a custom-designed mini heat chamber operating at a frequency of 2.45 GHz and microwave power ranging from 200 W to 700 W. The exposure time varied from 5 to 15 minutes. The heat chamber was appropriately positioned in a domestic microwave oven. Vickers microhardness measurements and X-ray diffraction (XRD) were analysed on the metal surface. The experimental findings showed the highest microhardness, 572 Hv at 700 W microwave power and heating time 15 minutes. The XRD spectrum detected formation of Fe₅C₂, Fe₉S₁₁, and Fe₄Al₁₃ presence on the steel's surface after heating. Meanwhile, the smallest grain size, 3.6 µm was found for samples heated at 700 W power and heating time 5 minutes under rapid cooling. Higher power and heating time have damaged the samples and cannot be used for further heating. The study concludes that as the microwave power increased for preheating, the microhardness of the steel G550 had increased. This study on microwave hybrid heating for steel G550 sheets addresses a critical need in industrial material processing. By investigating the effects of varying microwave power and exposure times, the research offers insights into optimizing preheating techniques. The findings hold promise for enhancing efficiency and quality in manufacturing processes, fostering innovation and sustainability in industry.

Keywords: MHH, zincalume steel, pre-heating, microhardness, microstructure

Article Info

Received 3rd January 2024 Accepted 25th March 2024 Published 12th June 2024

Copyright Malaysian Journal of Microscopy (2024). All rights reserved.

ISSN: 1823-7010, eISSN: 2600-7444

1. INTRODUCTION

Steel, a widely used material across industries due to its characterizations of high strength, toughness, and ductility [1]. Zincalume G550 refers to a coated steel material composed of approximately 55 % zinc and 45 % aluminum [2]. This specific composition provides Zincalume G550 steel with outstanding corrosion resistance, high tensile strength, excellent formability, and an attractive appearance. As a result, Zincalume G550 steel finds extensive application in the construction, automotive and manufacturing industries, where durability and corrosion resistance are paramount.

In recent years, numerous steel companies have significantly increased production of Zincalume steel, resulting in the generation of substantial volumes of waste. Therefore, this study aims to manage the generated waste more effectively and contribute to a sustainable environment by reducing industrial waste volumes. To achieve this, Zincalume G550 steel was pre-heated for welding lap joints using various parameters in microwave heating. To further enhance its performance and extend its mechanical life, steel often undergoes heat treatment processes [3]. Heat treatment techniques, including annealing, quenching, and tempering, offer the ability to modify the microstructure of steel, leading to significant improvements in its mechanical, physical, and chemical properties. These processes involve controlled heating and cooling cycles aimed at altering the crystal structure, dislocation density, grain size, and phase distribution within the steel, thereby influencing its hardness, strength, toughness, and other critical characteristics [4].

Nowadays, researchers have been investigating alternative methods of heat treatment to solve the issues of conventional techniques. The application of microwave or electromagnetic heating is one of the unique techniques for heat treatment purposes. Microwave heating employs high-frequency electromagnetic waves, while electromagnetic heating utilizes electromagnetic fields to directly generate heat within the material. These methods offer several advantages over traditional heat treatment techniques, including rapid and uniform heating rates, precise control of temperature distribution, reduced energy consumption, and enhanced process efficiency [5]. However, the reflection of microwave radiation by metallic materials is a critical consideration when applying microwave heating for various processes. Due to the unique electrical properties of metals, several reflection-related phenomena occur, which can impact the efficiency and effectiveness of the heating process [6]. Therefore, The Microwave Hybrid Heating (MHH) process is characterized by its ability to combine microwave heating with specific materials that can absorb and insulate from the electromagnetic wave, resulting in unique advantages.

MHH provides rapid and selective heating by leveraging the specific heating mechanisms of each method [7-8]. Moreover, MHH enables more uniform heating and temperature control throughout the material, overcoming challenges associated with non-uniform heating patterns. The process is flexible and adaptable, suitable for a wide range of materials and applications. It allows for improved process control and safety, with precise temperature monitoring and adjustment. The structures of MHH process includes microwave cave, magnetron, wave guide, susceptor, insulator and alumina brick or mask. Several researchers were investigating microwave hybrid heating (MHH) process that is used for metallurgical fields [9-10] was listed in Table 1.

Table 1: MHH technique for joint, sintering and cladding

Susceptor	Base	Exposure	Microwave	Used for	References
	material	time (min)	power (W)		
Charcoal	Copper	15	900	Joint	[11]
Charcoal	SS316	15	900	Joint	[12]
SiC	SS316	10	1200	Joint	[13]
Charcoal	Mild steel	10	900	Joint	[14]
SiC	Inconel-718	15	900	Joint	[15]
Charcoal	Inconel-625	21	900	Joint	[16]
SiC	Nickel alloy	60	200	Sintering	[17]
SiC	Copper alloy	30	300	Sintering	[18]
SiC	Aluminum	60	600	Sintering	[19]
	alloy			_	
SiC	SS-316	7	900	Cladding	[20]
SiC	SS304	10	1400	Cladding	[21]
SiC	SS316	15	900	Cladding	[22]

The Gamit, Mishra and Sharma [23] conducted at mild steel joint as the 900 W of microwave power and 480 s of exposure time using MHH process and it produced good microhardness at surface of metal. Negaraju, Kumaran and Rao [24] investigated microstructures behaviors in stainless-steel SS316 and SS304 under microwave sintering. In results, it found the exposure time is significantly to influence reduction size of grain and increasing of hardness and strength. Inconel 625 is successfully joined by MHH process at 900 W of microwave power and 21min of exposure time as a good strength and microhardness [25]. Aluminium alloy was sintered using the MHH technique at 800 W of microwave power and 15min of exposure time and aluminum oxide (Al₂O₃) and carbide were found in the XRD spectrum [26], and the Singh, Suri and Belokar [27] were found 72.4 HV of high microhardness in the joint of pure aluminum at 900W of microwave power and 600s of exposure time under the MHH process. SS316 was successfully sintered at 4.4kW and 60min of exposure time as the excellent strength and hardness using the MHH process [28]. However, the heat treated of steel-based materials as low power using MHH process has not been reported and studied yet. Therefore, the aim of this study is to investigate effectively heat treatment as low power and less exposure time using the unique designed MHH process and observing microstructures and microhardness.

2. MATERIALS AND METHODS

2.1 Materials

This study utilized a domestic microwave oven (Panasonic, capacity of 23 L) as a heating source, operating at a maximum microwave power of 900 W and a microwave frequency of 2.45 GHz. The parent metal consisted of Zincalume steel G550 sheets, with their chemical compositions provided in Table 2. Figure 1 presents a schematic diagram of the experimental

setup, including the dimensions of the specimen, which measured 20 x 20 x 0.6 mm. Prior to heating, the specimen's surface was thoroughly cleaned to remove any dust particles.

Table 2: Chemical compositions of parent metal

Element	C	Mn	S	P	Si	Al	Fe
Percentage	0.02-0.07	0.14-0.22	0.01-0.02	0.01-0.02	0-0.02	0.03-0.06	Bal.
(wt.%)							



Figure 1: Schematic diagram for sample

2.2 Heating Method

The Zincalume steel G550 underwent MHH processing, characterized by high heat rates. The experimental testing employed the aforementioned domestic microwave oven. The range of experimental and patterned design parameters can be found in Table 3 and Table 4.

Table 3: Experimental parameters setting

Parameters	Descriptions
Microwave frequency (GHz)	2.45
Cavity Capacity (L)	23
Microwave power (W)	200, 360 and 700
Susceptor materials	Active Graphite
Insulator material	Fused Quartz
Dimensions of specimen	20×20×0.6 mm
Exposure time (min)	5, 10 and 15

Table 4: Patterned design for parameters

Trial	Microwave power (W)	Exposure time (min)	
1	200	5	
2	200	10	
3	200	15	
4	360	5	
5	360	10	
6	360	15	
7	700	5	
8	700	10	
9	700	15	

In addition, the heat chamber played a crucial role in MHH processing, as depicted in Figure 2(a) to (c) and Figure 3. The heat chamber comprised several key components, including an active graphite (absorber), fused quartz (insulator and microwave-transparent material), a metal conductor (for conduction heating), a clamp, and an alumina brick. Within the six sandwich layers composed of active graphite and fused quartz, plasma was generated and observed. Microwave radiation was fully absorbed by the interaction between the active graphite and fused quartz, resulting in the formation of clouds of electrons or electric arcs. The electric arcs were channeled to the metal conductor, transmitting high heating energy to the specimens, which were covered with graphite chips to facilitate rapid heating.

This innovative MHH technique facilitated effective joint formation at low microwave power, as illustrated in Figure 4, depicting heat transfer at various microwave power levels such as 200, 270 and 360 W. Moreover, the sandwich layers provided comprehensive masking along the boundaries and edges of the specimens, ensuring minimal heat loss.

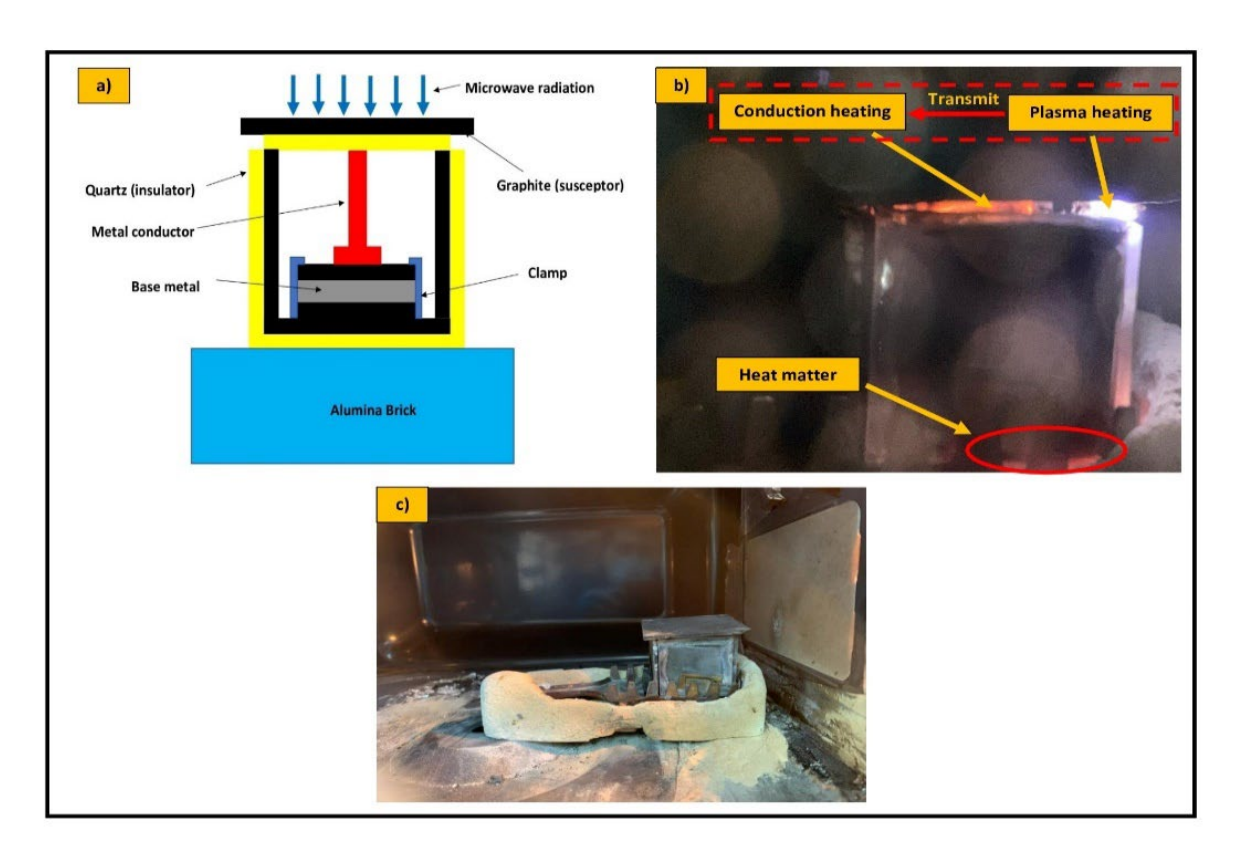


Figure 2: Schematic diagram for MHH processing (a) heat chamber parameters, (b) heating definition and (c) heat chamber setting

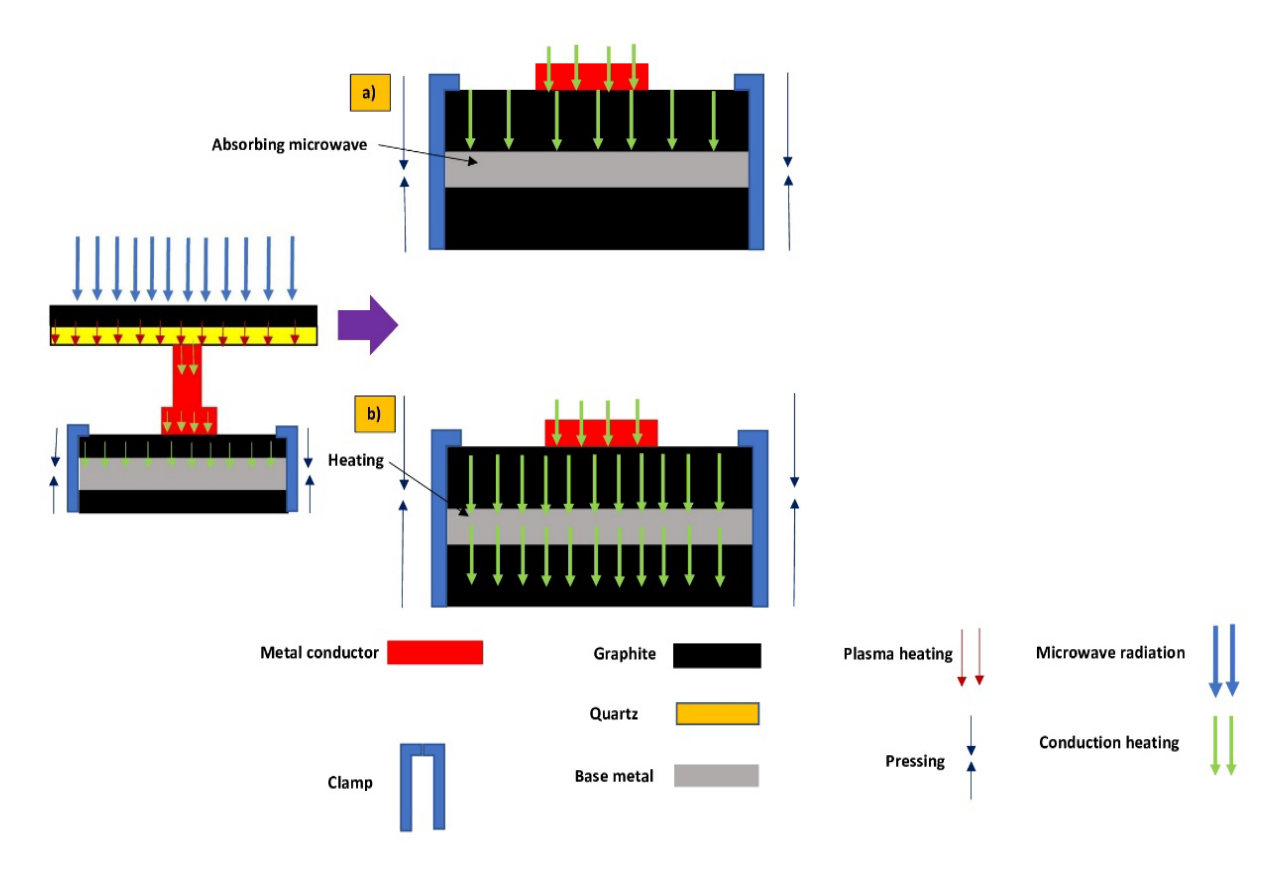


Figure 3: Heating mechanisms in MHH process (a) microwave absorption and (b) heating

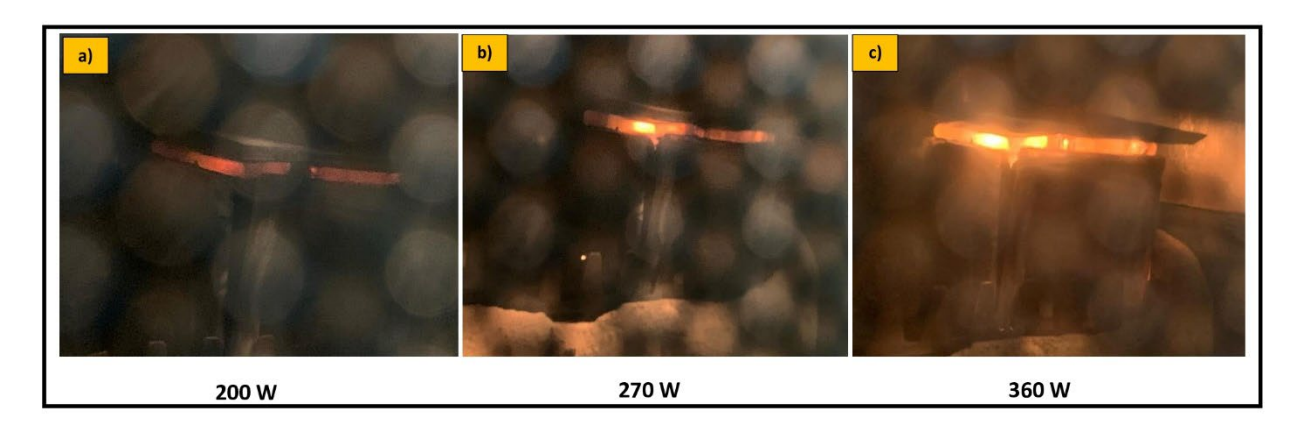


Figure 4: Microwave power for heat transfer process (a) 200 W, (b) 270 W and (c) 360 W

2.3 Metallurgical Characterizations

In this study, the specimens subjected to heating were initially cold mounted using an epoxy to hardener ratio of 25:10, respectively. The heated section cuts were examined using multiple analytical techniques, including scanning electron microscopy (SEM) with a resolution of 5 mm, X-ray diffraction (XRD), and Vickers hardness testing with a 5 mm indenter. Subsequently, the cut specimens underwent grinding using different grades of grit papers (220,

1000, and 2000) followed by polishing with diamond suspension. Figure 5 illustrates the schematic diagram for heating characterization. To reveal the alpha grain structure of the heated surface, an etching process was performed using a ferric chloride (FeCl₃) solution. The microstructure of the cross-sectioned joint surface was evaluated using an SEM machine (HITACHI, JSM-7800F). The microhardness of the joint surface was measured using a Vickers hardness machine (Model HV-1000A) at five different spots on the base metal, applying a load of 0.05 kg for a dwell time of 15 seconds. Figure 6 presents the schematic diagram depicting the distribution of hardness. The chemical components present in the joint region were analyzed using an XRD solution (Empyrean, PANalytical).

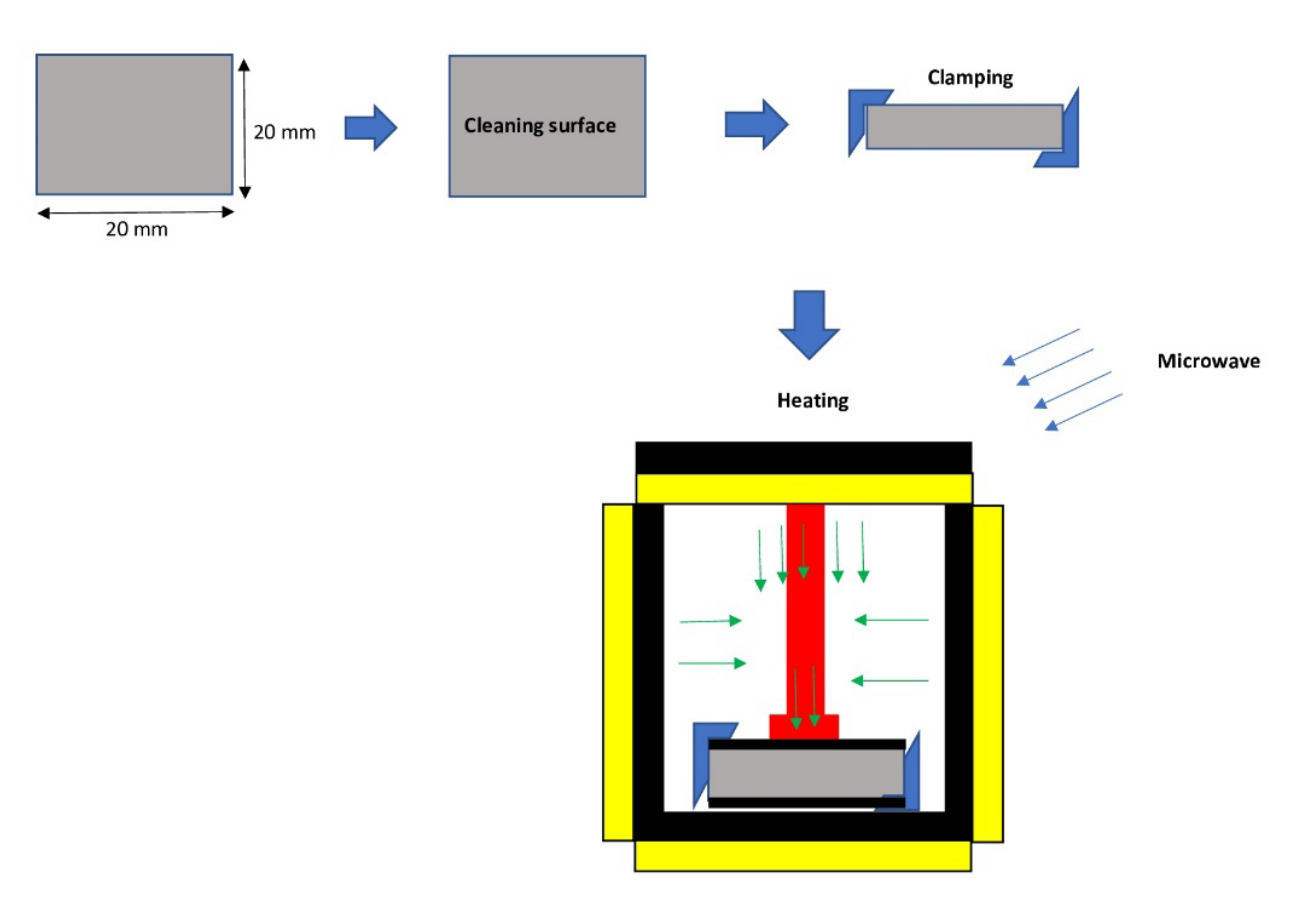


Figure 5: Schematic diagram for heating characterization

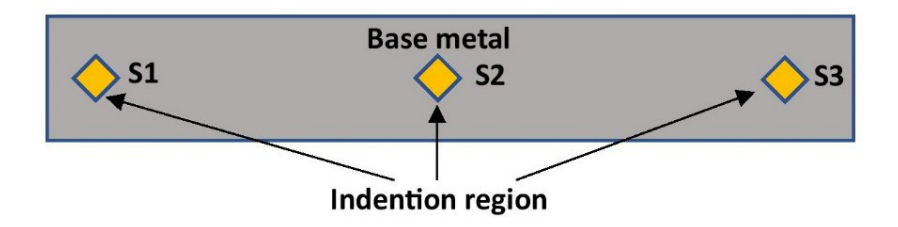


Figure 6: Hardness distribution

3. RESULTS AND DISCUSSION

3.1 Analysis of Microhardness

The microhardness testing revealed distinct variations in hardness values across the different heat treatment parameters such as microwave power (ranges from 200 to 700 W) and exposure time (ranges from 5 to 15 min) as shown in Table 5 and Figure 7. The maximum hardness of 572 HV was achieved at 700 W and 15 min of exposure time, representing the most favorable combination of parameters. In contrast, the minimum hardness of 110.2 HV was observed at 200 W and 5 min of exposure time. The microstructural changes induced by microwave heat treatment significantly influence the resulting microhardness values. At the high microwave power and exposure time (700 W and 15 min), it is expected that the heat treatment led to a refined microstructure characterized by fine grain size, homogeneous phase distribution, and potential precipitation of strengthening phases. It is shown in SEM images in Figure 8. These microstructural features contribute to increased hardness through mechanisms such as grain boundary strengthening (reducing grain size) and solid solution strengthening [29]. Conversely, at the low microwave power and exposure time (200 W and 5 min), a coarser microstructure with larger grain size and less defined phase distribution is anticipated. This coarser microstructure results in reduced hardness due to limited strengthening effects. The correlation between microhardness values and microstructural features, such as coarse grains, confirms that microwave heating parameters influence resulting hardness values, which decrease as grain size increases [30]. The refined microstructure achieved at 700 W and 15 min exhibits improved microhardness due to enhanced grain boundary (reducing grain size) and solid solution strengthening mechanisms. In contrast, the coarser microstructure obtained at 200 W and 5 min results in lower hardness values. These findings highlight the importance of optimizing the heat treatment parameters to achieve desired microstructural characteristics and corresponding hardness properties.

Table 5: Results for microhardness

Trial No.	Microwave power (W)	Exposure time (min)	S1	S2	S2	Microhardness (HV)	Stdev
1	200	5	100.7	121.1	108.8	110.2	10.2718
2	200	10	150.6	153.3	147	150.3	3.1607
3	200	15	130.9	168.8	137.6	145.8	20.2268
4	360	5	107.4	127.2	126.5	120.4	11.2349
5	360	10	117.4	131.8	119.1	122.8	7.86914
6	360	15	218.6	338	143	233.2	98.3164
7	700	5	419	434.2	415.5	422.9	9.94133
8	700	10	381.1	662.2	567.5	536.9	143.021
9	700	15	529.3	593.4	593.4	572	37.0082

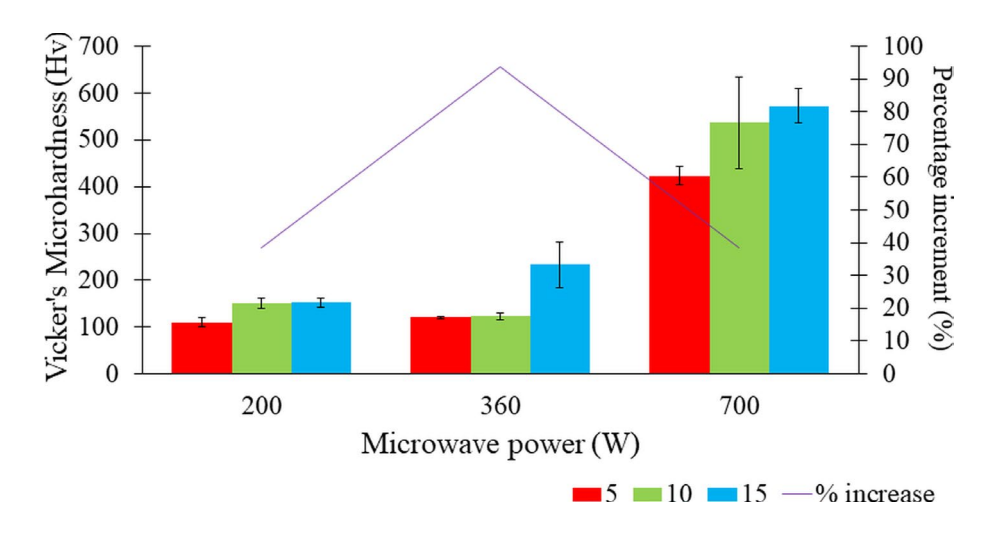


Figure 7: Vicker's microhardness analysis for time increment of 5 minutes

3.2 Analysis of Microstructure

The microstructure analysis using scanning electron microscopy (SEM) revealed important insights into the effects of microwave hybrid heating on the microstructural characteristics of Zincalume steel (G550) with varied exposure times (5, 10 and 15 min) at a constant microwave power of 360 W as shown in Figure 8(a) to (c). The presence and distribution of a-ferrite and Carbide phases were observed, along with variations in grain size. One significant observation from the analysis is the relationship between exposure time and grain size. As the exposure time increased, there was a clear trend of decreasing grain size. This can be attributed to the increased diffusion and transformation rates facilitated by longer exposure times under microwave hybrid heating. The higher energy input and longer duration allow for more effective homogenization and grain refinement processes, resulting in finer grains. Conversely, shorter exposure times limit the extent of microstructural changes, leading to the presence of coarser grains. The distribution of a-ferrite and Carbide phases within the microstructure varied with both exposure time and grain size. In Figure 8(a) to (b), coarse grains exhibited a higher concentration of a-ferrite, indicating the presence of a larger fraction of this phase in regions with slower cooling rates (air cooling). The slower cooling rates associated with larger grain sizes promote the formation and stabilization of a-ferrite.

On the other hand, medium-coarse grains displayed a more balanced distribution of aferrite and Carbide, suggesting a transition region between the two phases [31]. The increased presence of Carbide in fine grains indicates that finer grain sizes favor the formation and precipitation of Carbide during the heat treatment process. These findings highlight the influence of exposure time and grain size on the microstructural evolution of Zincalume steel under microwave hybrid heating. The ability to control grain size through exposure time manipulation offers potential benefits in tailoring the material's mechanical and thermal properties. Finer grain sizes are associated with improved mechanical hardness and strength, enhanced formability, and increased resistance to crack propagation. Therefore, longer exposure times can be utilized to achieve finer grain structures and optimize the desired material properties for specific

applications. It is worth noting that this study focused on the microstructural analysis of Zincalume steel under microwave hybrid heating.

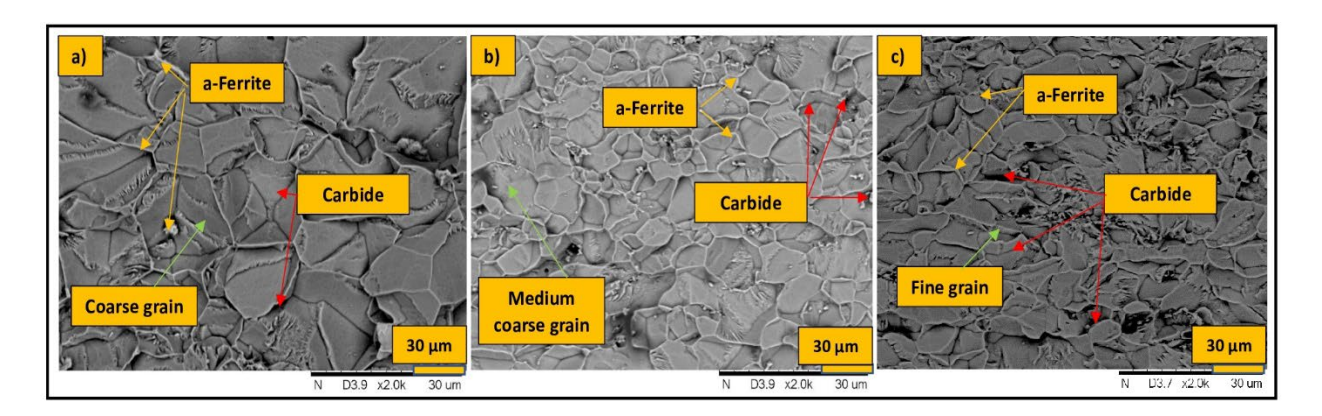


Figure 8: SEM images for heat treatment of Zincalume G550 under variety of exposure time a) 5 min, b) 10 min and c) 15 min at constant 360 W of microwave power in scale of 30 μm.

In this study also investigated and observed to explore the mechanical properties, such as microhardness of the heat-treated samples to provide a comprehensive understanding of the material's performance as referred to Figure 7. Additionally, thermal properties, including thermal conductivity and coefficient of thermal expansion, should be assessed to evaluate the impact of microwave hybrid heating on heat transfer characteristics. In summary, the microstructure analysis using SEM revealed that increasing exposure time under microwave hybrid heating resulted in a decrease in grain size. The distribution of a-ferrite and Carbide phases varied with exposure time and grain size, with coarser grains exhibiting a higher concentration of a-ferrite, medium-coarse grains showing a balanced distribution, and fine grains displaying an increased presence of Carbide [32-33]. These findings contribute to the understanding of microwave-assisted heat treatment of Zincalume steel and provide insights for optimizing its microstructure and subsequent material properties.

3.3 Calculation of Grain Size

The microstructural analysis conducted through SEM, grain size calculations provide valuable quantitative data to further understand the impact of microwave hybrid heating on Zincalume steel (G550). In this study, the linear method and equation were employed to determine the grain size (L) in the heat-treated samples as Equation (1).

$$L = \frac{L_0}{N \times M} \tag{1}$$

where L0 represents total represented area is measured by ImageG software, N is numbers of grain boundary and M is representing magnification of image.

The grain size calculations revealed that the exposure time and microwave power had a significant effect on the resulting grain size as shown in Figure 9. As the exposure time increased from 5 min to 15 min, and the microwave power increased from 360 W to 700 W, there was a

consistent trend of decreasing grain size. At 5 min of exposure time and 360W microwave power, the calculated grain size was determined to be 9.3 µm. This indicates that a relatively short exposure time and lower microwave power resulted in larger grain sizes.

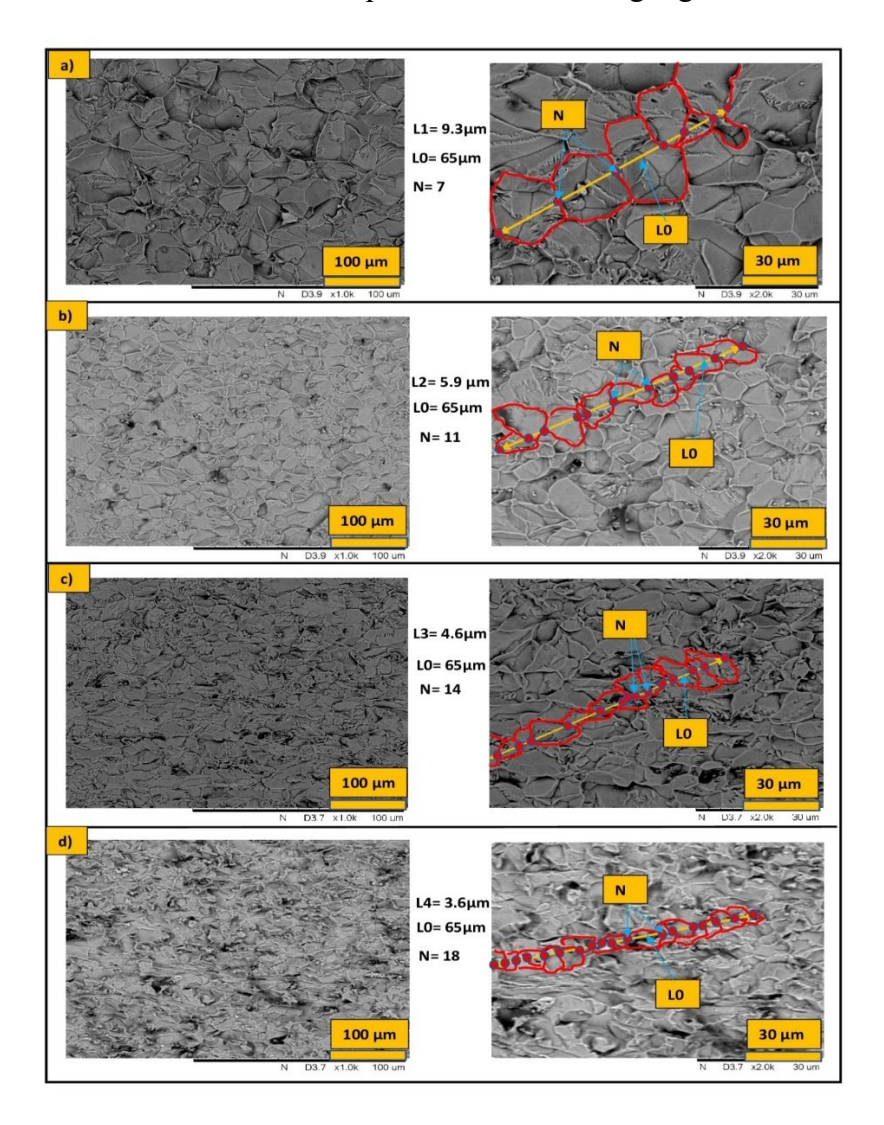


Figure 9: SEM images for microstructure and grain size (a) at 360 W, 5 min, (b) at 360 W, 10 min, (c) at 360 W, 15 min and (d) at 700 W, 5 min. L1-L4: grain's length, L0: total length of selected area and N: numbers of grain boundary

As exposure time increased to 10 min and 15 min, with the same microwave power, the grain size decreased to 5.9 µm and 4.6 µm, respectively. This suggests that longer exposure times allowed for more efficient diffusion and transformation processes, leading to grain refinement. Furthermore, when the microwave power was increased to 700 W while maintaining a constant exposure time of 5 min, the grain size decreased further to 3.6 µm. The higher microwave power likely provided increased energy input, promoting faster heating and enhancing the diffusion and transformation rates within the material [34]. Consequently, the combination of longer exposure time and higher microwave power resulted in the smallest grain size observed in the study. These findings demonstrate that both exposure time and microwave power have significant influences

on grain size in Zincalume steel under microwave hybrid heating. Longer exposure times and higher microwave powers facilitate the reduction of grain size through increased diffusion and transformation rates under rapid cooling. The combination of these factors results in more refined microstructures, which often exhibit improved mechanical properties, such as increased strength and hardness.

3.4 Analysis of XRD at Heated Interface of Zincalume Steel

The X-ray diffraction (XRD) analysis provides valuable insights into the phase composition and crystal structure of the interface of Zincalume steel (G550) subjected to microwave hybrid heating. In this study, the XRD spectrum detected the presence of Fe₅C₂, Fe₉S₁₁, and Fe₄Al₁₃ as the 65, 6.9, and 44.7° at the 2θ on the surface of Zincalume steel after 5 min of exposure time at 360 W of microwave power as shown in Figure 10. The formation of these chemical compounds can be influenced by the heat temperature during the treatment process. The heat temperature plays a crucial role in phase transformations and chemical reactions occurring in the material. The interaction between the microwave energy and the Zincalume steel leads to localized heating, resulting in elevated temperatures at the surface. These increased temperatures facilitate diffusion and reaction kinetics, ultimately influencing the formation of specific compounds. Fe₅C₂ (iron carbide) is known to form under conditions of elevated temperature and carbon-rich environments. During the heat treatment process, the elevated temperature allows for the diffusion of carbon within the steel matrix. Carbon atoms can react with iron, leading to the formation of Fe₅C₂. Higher heat temperatures can promote enhanced carbon diffusion, potentially increasing the concentration and promoting the formation of Fe₅C₂ [35]. Similarly, Fe₄Al₁₃ (iron sulfide) formation is influenced by the heat temperature. Sulfur, an impurity or environmental contaminant, can react with iron at elevated temperatures to form iron sulfides [36].

The heat treatment process provides the necessary thermal energy for the diffusion of sulfur and its subsequent reaction with iron, resulting in the formation of Fe₉S₁₁ [37]. The temperature range and the duration of exposure to these temperatures are crucial in determining the extent of Fe₉S₁₁ formation. Fe₄Al₁₃ (iron aluminide) formation is also temperature dependent. Iron aluminides typically form when aluminum diffuses into the iron matrix and reacts with iron. The elevated heat temperature during the heat treatment process enables the diffusion of aluminum and promotes the formation of Fe₄Al₁₃. Higher heat temperatures can enhance the kinetics of the diffusion process, resulting in increased aluminum incorporation and subsequent Fe₄Al₁₃ formation. It is important to note that the specific heat temperature required for the formation of Fe₅C₂, Fe₉S₁₁, and Fe₄Al₁₃ can vary depending on the alloy composition, impurities, and processing conditions. Optimization of the heat treatment parameters, including temperature and duration, is essential to achieve the desired phase compositions and microstructural characteristics. The microhardness properties of the heat-treated Zincalume steel can be influenced by the formation of these chemical compounds. Iron carbides and iron aluminides generally exhibit higher hardness compared to the base metal, potentially leading to an increase in microhardness [38]. On the other hand, the presence of iron sulfides may have varying effects on microhardness, depending on their concentration, morphology, and distribution within the material [39].

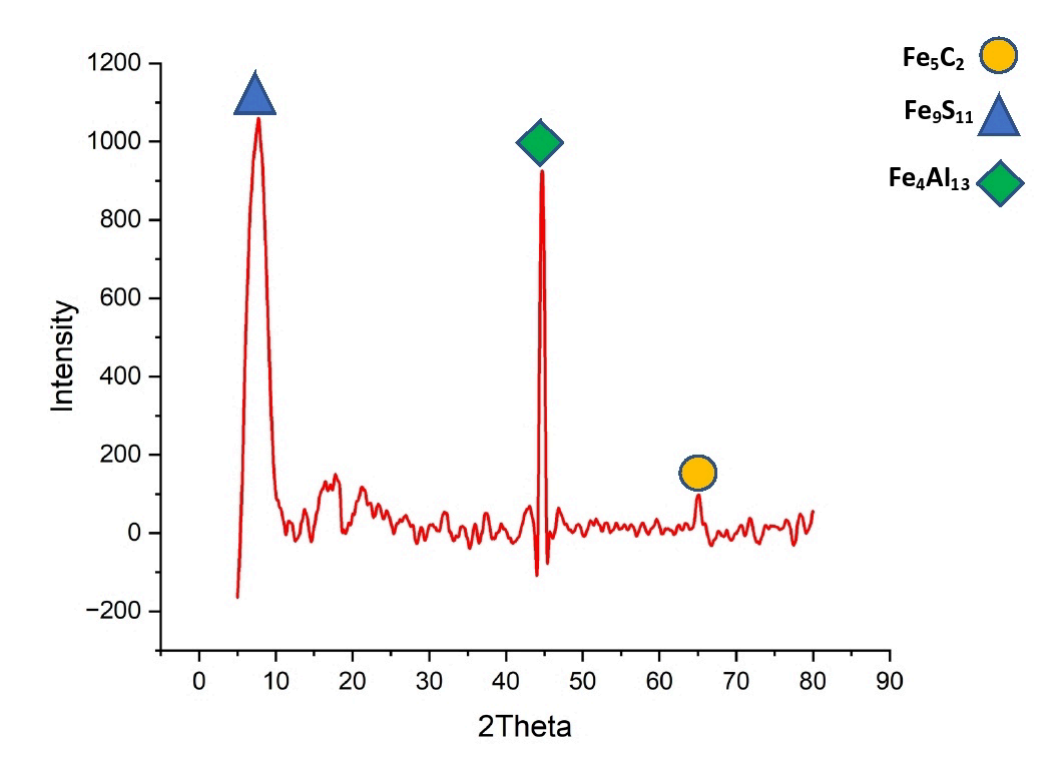


Figure 10: XRD spectrum for heat treated at 5 min of exposure time and 360W of microwave power

4. CONCLUSIONS

The preheating of steel G550 using the microwave hybrid heating (MHH) process was investigated, focusing on the evaluation of microhardness measurements and XRD analysis. Following are the conclusion made:

- The MHH process can significantly influence the microhardness of steel G550. A maximum microhardness value of 572 Hv was achieved when employing a microwave power of 700 W and an exposure time of 15 minutes. This notable increase in microhardness can be attributed to the improved heating efficiency and uniformity provided by the MHH technique.
- XRD analysis conducted on cross-sectional samples found the presence of Fe₅C₂, Fe₉S₁₁, and Fe₄Al₁₃ phases, indicating potential phase transformations induced by the MHH process. These phase changes can further contribute to the enhancement of material properties and structural integrity.
- Formation of small grains happens as the heating increases with increasing of time.

Acknowledgements

This research was supported in part by the from grant number: SEGiIRF/2022-Q1/FoEBEIT/001

Author Contributions

All authors contributed toward data analysis, drafting and critically revising the paper and agree to be accountable for all aspects of the work.

Disclosure of Conflict of Interest

The authors have no disclosures to declare.

Compliance with Ethical Standards

The work is compliant with ethical standards.

References

- [1] Kong, D., Dong, C., Ni, X., Zhang, L., Yao, J., Man, C., Cheng, X., Xiao, K. and Li, X. (2019). Mechanical properties and corrosion behavior of selective laser melted 316L stainless steel after different heat treatment processes. *Journal of Materials Science & Technology*. 35(7), 1499-1507.
- [2] Tayier, W., Janasekaran, S., & Vijayasree, V. P. (2022). Evaluation of heat input and bead geometry of zincalume steel (G550) welded joint between metal inert gas (MIG) and laser beam welding (LBW). *Materials Today: Proceedings.* 48, 895-904.
- [3] Kishore, K., Kumar, P., & Mukhopadhyay, G. (2021). Microstructure, tensile and fatigue behaviour of resistance spot welded zinc coated dual phase and interstitial free steel. *Metals and Materials International*. 1-21.
- [4] Mubarak, N. M., Anwar, M., Debnath, S., & Sudin, I. (2023). Fundamentals of Biomaterials: A Supplementary Textbook. Springer Nature.
- [5] Lingappa, S. M., Srinath, M. S., & Amarendra, H. J. (2019). Melting of bulk non-ferrous metallic materials by microwave hybrid heating (MHH) and conventional heating: a comparative study on energy consumption. *Journal of the Brazilian Society of Mechanical Sciences and Engineering*. 40, 1-11.

- [6] Badiger, R. I., Narendranath, S., & Srinath, M. S. (2018). Microstructure and mechanical properties of Inconel-625 welded joint developed through microwave hybrid heating. *Proceedings of the Institution of Mechanical Engineers, Part B: Journal of Engineering Manufacture*. 232(14), 2462-2477.
- [7] Tamang, S., & Aravindan, S. (2021). Effect of susceptors on joining of AA6061-T6 to AZ31B by microwave hybrid heating. *Journal of Materials Engineering and Performance*. 1-10.
- [8] Pal, M., Kumar, V., Sehgal, S., Kumar, H., Saxena, K. K., & Bagha, A. K. (2021). Microwave hybrid heating based optimized joining of SS304/SS316. *Materials and Manufacturing Processes*. 36(13), 1554-1560.
- [9] Naik, S. R., Gadad, G. M., & Hebbale, A. M. (2021). Joining of dissimilar metals using microwave hybrid heating and Tungsten Inert Gas welding-A review. *Materials Today: Proceedings.* 46, 2635-2640.
- [10] Badiger, R. I., Narendranath, S., & Srinath, M. S. (2019). Optimization of process parameters by Taguchi grey relational analysis in joining Inconel-625 through microwave hybrid heating. *Metallography, Microstructure, and Analysis.* 8, 92-108.
- [11] Srinath, M. S., Sharma, A. K., & Kumar, P. (2020). A new approach to joining of bulk copper using microwave energy. *Materials & Design*. 32(5), 2685-2694.
- [12] Srinath, M. S., Sharma, A. K., & Kumar, P. (2021). A novel route for joining of austenitic stainless steel (SS-316) using microwave energy. *Proceedings of the Institution of Mechanical Engineers, Part B: Journal of Engineering Manufacture.* 225(7), 1083-1091.
- [13] Bansal, A., Sharma, A. K., Kumar, P., & Das, S. (2019). Characterization of bulk stainless steel joints developed through microwave hybrid heating. *materials characterization*. 91, 34-41.
- [14] Srinath, M. S., Sharma, A. K., & Kumar, P. (2018). A new approach to joining of bulk copper using microwave energy. *Materials & Design*. 32(5), 2685-2694.
- [15] Bansal, A., Sharma, A. K., & Das, S. (2019). Metallurgical and mechanical characterization of mild steel-mild steel joint formed by microwave hybrid heating process. *Sadhana*. 38, 679-686.
- [16] Dwivedi, S. P., & Sharma, S. (2017). Effect of process parameters on tensile strength of 1018 mild steel joints fabricated by microwave welding. *Metallography, Microstructure, and Analysis*. 3, 58-69.
- [17] Tang, C. Y., Zhang, L. N., Wong, C. T., Chan, K. C., & Yue, T. M. (2018). Fabrication and characteristics of porous NiTi shape memory alloy synthesized by microwave sintering. *Materials Science and Engineering: A.* 528(18), 6006-6011.

- [18] Liu, R., Hao, T., Wang, K., Zhang, T., Wang, X. P., Liu, C. S., & Fang, Q. F. (2018). Microwave sintering of W/Cu functionally graded materials. *Journal of nuclear materials*. 431(1-3), 196-201.
- [19] Padmavathi, C., Upadhyaya, A., & Agrawal, D. (2019). Microwave assisted sintering of Al-Cu-Mg-Si-Sn alloy. *Journal of Microwave Power and Electromagnetic Energy*. 46(3), 115-127.
- [20] Gupta, D., & Sharma, A. K. (2019). Copper coating on austenitic stainless steel using microwave hybrid heating. *Proceedings of the Institution of Mechanical Engineers, Part E: Journal of Process Mechanical Engineering.* 226(2), 132-141.
- [21] Hebbale, A. M., & Srinath, M. S. (2020). Microstructural investigation of Ni based cladding developed on austenitic SS-304 through microwave irradiation. *Journal of materials research and technology*. 5(4), 293-301.
- [22] Gupta, D., Bhovi, P. M., Sharma, A. K., & Dutta, S. (2019). Development and characterization of microwave composite cladding. *Journal of manufacturing processes*. 14(3), 243-249.
- [23] Gamit, D., Mishra, R. R., & Sharma, A. K. (2017). Joining of mild steel pipes using microwave hybrid heating at 2.45 GHz and joint characterization. *Journal of Manufacturing Processes*. 27, 158-168.
- [24] Nagaraju, K. V. V., Kumaran, S., & Rao, T. S. (2021). Electrochemical behavior of various grade P/M stainless steels processed by rapid microwave hybrid sintering (super-solidus) method. *Materials Letters*. 302, 130394.
- [25] Badiger, R. I., Narendranath, S., & Srinath, M. S. (2018). Joining of inconel-625 alloy through microwave hybrid heating and its characterization. *Journal of Manufacturing Processes*. 18, 117-123.
- [26] Singhal, C., Murtaza, Q., Alam, P., & Hasan, F. (2019). Structural and mechanical properties of microwave hybrid sintered aluminium silicon carbide composite. *Advances in Materials and Processing Technologies*. 5(4), 559-567.
- [27] Singh, S., Suri, N. M., & Belokar, R. M. (2019). Characterization of joint developed by fusion of aluminum metal powder through microwave hybrid heating. *Materials Today: Proceedings*. 2(4-5), 1340-1346.
- [28] Nagaraju, K. V. V., Kumaran, S., & Rao, T. S. (2020). Microwave sintering of 316L stainless steel: Influence of sintering temperature and time. *Materials Today: Proceedings*. 27, 2066-2071.
- [29] Salman, O. O., Gammer, C., Chaubey, A. K., Eckert, J., & Scudino, S. (2019). Effect of heat treatment on microstructure and mechanical properties of 316L steel synthesized by selective laser melting. *Materials Science and Engineering: A.* 748, 205-212.

- [30] Deng, Y. G., Li, Y., Di, H., & Misra, R. D. K. (2019). Effect of heating rate during continuous annealing on microstructure and mechanical properties of high-strength dual-phase steel. *Journal of Materials Engineering and Performance*. 28, 4556-4564.
- [31] Ghorabaei, A. S., & Nili-Ahmadabadi, M. (2021). Effects of prior austenite grain size and phase transformation temperature on bainitic ferrite formation in multi-constituent microstructures of a strong ultra-low-carbon steel. *Materials Science and Engineering: A.* 815, 141300.
- [32] Lan, L., Qiu, C., Zhao, D., Gao, X., & Du, L. (2018). Microstructural characteristics and toughness of the simulated coarse grained heat affected zone of high strength low carbon bainitic steel. *Materials Science and Engineering: A.* 529, 192-200.
- [33] Cui, J., Zhu, W., Chen, Z., & Chen, L. (2020). Microstructural characteristics and impact fracture behaviors of a novel high-strength low-carbon bainitic steel with different reheated coarse-grained heat-affected zones. *Metallurgical and Materials Transactions A*. 51, 6258-6268.
- [34] Tian, J., Xu, G., Zhou, M., Hu, H., & Wan, X. (2020). The effects of Cr and Al addition on transformation and properties in low-carbon bainitic steels. *Metals*. 7(2), 40.
- [35] Wang, D., Cao, J. C., Zhou, X. L., Zhao, D. W., & Deng, L. (2019). First-principles calculation of carbides in niobium microalloyed medium and high carbon steels. *Advanced Materials Research*. 468, 1798-1801.
- [36] Zedan, M. J., & Doos, Q. M. (2018). New method of resistance spot welding for dissimilar 1008 low carbon steel-5052 aluminum alloy. *Procedia Structural Integrity*. 9, 37-46.
- [37] Wesley, W. (2023). Synthesis, Characterization and Applications of Metal Oxide and Sulfide Nanostructures (Doctoral dissertation, State University of New York at Stony Brook).
- [38] Vilardell, A. M., Cinca, N., Tarrés, E., & Kobashi, M. (2022). Iron aluminides as an alternative binder for cemented carbides: A review and perspective towards additive manufacturing. *Materials Today Communications*, 31, 103335.
- [39] Chareev, D. A., Osadchii, V. O., Shiryaev, A. A., Nekrasov, A. N., Koshelev, A. V., & Osadchii, E. G. (2017). Single-crystal Fe-bearing sphalerite: synthesis, lattice parameter, thermal expansion coefficient and microhardness. *Physics and Chemistry of Minerals*. 44, 287-296.